J. Membrane Biol. 127, 95–111 (1992)

The Journal of
Membrane Biology

Multiple-Channel Conductance States and Voltage Regulation of Embryonic Chick Cardiac Gap Junctions

Yan-hua Chen and Robert L. DeHaan
Department of Anatomy and Cell Biology, Emory University Health Science Center, Atlanta, Georgia 30322

Summary. We used the double whole-cell voltage-clamp technique on ventricle cell pairs isolated from 7-day chick heart to measure the conductance of their gap junctions (G_j) and junctional channels (γ_j) with a steady-state voltage difference (V_j) applied across the junction. Currents were recorded from single gap junction channels (i_j) as symmetrical rectangular signals of equal size and opposite sign in the two cells, and γ_j was measured from i_j/V_j. We observed channel openings at six reproducible conductance levels with means of 42.6, 80.7, 119.6, 157.7, 200.4 and 240.3 pS. More than half of all openings were to the 80- and 160-pS conductance levels. The probability that a high conductance event (e.g., 160 or 240 pS) results from the random simultaneous opening of several 40-pS channels is small, based on their frequency of occurrence and on the prevalence of shifts between small and large conductance states with no intervening 40-pS steps. Our results are consistent with three models of embryonic cardiac gap junction channel configuration: a homogeneous population of 40-pS channels that can open cooperatively in groups of up to six; a single population of large channels with a maximal conductance near 240 pS and five smaller substates; or several different channel types, each with its own conductance.

G_j was determined from the junctional current (I_j) elicited by rectangular pulses of applied transjunctional voltage as I_j/V_j. It was highest near 0 V_j and was progressively reduced by application of V_j between 20 and 80 mV or −20 and −80 mV. In response to increases in V_j, G_j decayed in a voltage- and time-dependent fashion. After a 6-sec holding period at 0 V_j, the initial conductance (G_{init}) measured immediately after the onset of an 80-mV step in V_j was nearly the same as that measured by a 10-mV prepulse. However, during 6-sec pulses of $V_j > \pm 20$ mV, G_j declined over several seconds from G_{init} to a steady-state value (G_{ss}). At potentials greater than ±20 mV the current decay could be fit with biexponential curves with the slow decay time constant (τ_2) 5–20 times longer than τ_1. For the response to a step to 80 mV V_j, for example, τ_1 = 127 msec and τ_2 = 2.6 sec. The rate of current decay in response to smaller positive or negative steps in V_j was slower, the magnitude of the decline was smaller, and the ratio τ_2/τ_1 decreased. The relationship between G_{init} and V_j was approximately linear between 0 and 80 mV or −80 mV, whereas the relationship between G_{ss} and V_j was nonlinear beyond ±20 mV. Upon returning to 0 V_j, G_j recovered with a biexponential time course, reaching its maximal value after several seconds; recovery time constants after a step in V_j from 80 to 0 mV were 225 msec and 1.9 sec. In the resting state, at low junctional voltage, high conductance channel activity (160–240 pS) is favored. Voltage-dependent decline of G_j results in part from a shift from high to lower conductance states.

Key Words gap junctions · ion channels · heart · patch-clamp technique

Introduction

The cardiac myocytes of heart muscle are connected by gap junctions that allow rapid impulse transmission from cell to cell and account for the near synchrony of beat in the different cardiac regions (DeHaan et al., 1981; Page & Manjunath, 1986; Spray & Burt, 1990). The conductance of gap junctions is sensitive to a wide variety of agents, including $[Ca]_i$, $[pH]_i$, temperature, long chain alcohols, and factors that regulate protein phosphorylation (Loewenstein, 1981; DeHaan, Chen & Penrod, 1989; Musil, Beyer & Goodenough, 1990; Spray & Burt, 1990). In adult heart, gap junction channels are insensitive to both inside-out membrane potential and transjunctional voltage (V_j) (e.g., Noma & Tsuboi, 1987). In contrast, voltage-sensitive junctional behavior has been reported in pairs of cardiac myocytes from chick embryo (Chen, Penrod & DeHaan, 1988; DeHaan et al., 1989; Veenstra, 1990*a-c*) and mammalian neonatal heart (Rook, Jongsma & van Ginneken, 1988; Veenstra, 1990*a*). The voltage response in these cells resembles the voltage and time dependence that characterizes the junctions that connect the blastomeres of amphibian and fundulus embryos (Spray, Harris & Bennett, 1981; Ebihara et al., 1989; Spray et al., 1990) but is less steep. The conductance of gap junctions in pairs of 7-day chick embryo ventricular cells is voltage dependent in the V_j range between 20 and 80 mV and −20 and −80 mV (Chen et al., 1988; DeHaan et al., 1989; Veenstra, 1990*a-c*). Application of a step of transjunctional voltage greater than ±20 mV caused junctional conductance (G_j) to

decay exponentially to a low steady-state value in 5–6 sec. Upon return to a V_j near 0 mV, G_j recovered to its original level over a similar time course. These observations suggest that resting gap junction channels (i.e., with no applied V_j) have a high conductance during embryonic development. They also indicate that resting G_j can be measured accurately and with little perturbation by applying pulses of V_j smaller than ±20 mV.

In the present work we confirm the existence of multiple-channel conductances in embryonic cardiac gap junctions and explore their role in the time- and voltage-dependent decay of G_j. Pairs of neonatal rat heart cells have junctional channels with γ_j near 20 and 40–50 pS (Rook et al., 1988; Rook, Jongsma & de Jonge, 1989; Spray & Burt, 1990). In contrast, we demonstrated in early experiments that the channels of embryonic chick heart gap junctions had two much larger conductance levels near 80 and 160 pS. These observations were from spontaneous channel open-close events that occurred in the steady state with V_j held constant for many minutes at 40 mV (Veenstra & DeHaan, 1988). More recently, under slightly different conditions, we recorded four major conductance levels near 40, 80, 160, and 240 pS (DeHaan, 1988; Chen & DeHaan, 1989; DeHaan et al., 1989). In the present paper, we confirm the 240-pS conductance state and the three original smaller conductances. We also report two additional levels at 120 and 200 pS. These results are consistent with three models: cooperative gating of a homogeneous population of 40-pS channels, a homogeneous population of large (240-pS) channels that have five smaller substates in increments of 40 pS, or the existence of several different channel classes. These models are discussed below and reviewed in detail in Chen and DeHaan (1992). During a step in V_j to a level such as 80 mV that causes a prominent current decay, the opening of channels with larger conductances becomes less frequent while smaller levels remain active.

Materials and Methods

Culture Technique

Ventricles of 7-day chick embryo hearts were dissociated into suspensions that included single cells, pairs, and cell clusters, using the 4-cycle trypsinization procedure now routine in this laboratory (Fujii, Ayer & DeHaan, 1988). The cells were suspended in culture medium 21212 and plated in glass slide chambers (0.5-ml capacity) which had been treated with concentrated sulfuric acid (18 M) to adjust the adhesiveness of the surface to allow cells to attach without flattening (Fujii et al., 1988). The cultures were prepared at a density of 1×10^5 cells/chamber and incubated at 37°C in an atmosphere of 85% N_2, 10% O_2, 5% CO_2 (pH = 7.4).

Table 1. Pipette solutions used for whole-cell recording

	IPS#57 (mM)	IPS#66 (mM)
CsCl	—	130
K-glutamate	120	—
NaCl	15	—
KH_2PO_4	1	—
$MgCl_2 \cdot 6H_2O$	4	4
$CaCl_2 \cdot 2H_2O$	4.7	0.068
EGTA	5	10
HEPES	10	5
Na_2ATP	3	3
Na_2PC	3	3
Free $[Ca]_i$*	1×10^{-6} M	$<1 \times 10^{-8}$ M

*Calculated according to Godt and Lindley (1982).

Solutions

Culture medium 21212 contained (by volume): 25% M199, 2% heat-inactivated horse serum, 4% fetal bovine serum, 67.5% K^+-free Ham's F12 (all from GIBCO, Grand Island, NY), 1% L-glutamine, 0.5% pen-G (Sigma Chemical) and 1.3 mM KCl. The external bath solution (DBS) used for electrophysiological recordings was composed of (in mM): NaCl 142; KCl 1.3; $MgSO_4$ 0.8; NaH_2PO_4 0.9; $CaCl_2$ 1.8; dextrose 5.5; and HEPES 10 (Baker Chemical, Phillipsburg, NJ). The pH was titrated to 7.4 by the addition of 1 N NaOH. The internal pipette solutions (IPS) used for whole-cell recording are shown in Table 1. IPS#57 and IPS#66 were calculated (Godt & Lindley, 1982) to buffer internal free $[Ca^{2+}]_i$ to high and low levels, respectively. CsCl was used in most experiments with IPS#66 instead of K-glutamate. The conductance of gap junction channels to the two cations is equal (Brink & Fan, 1989), and solutions containing the latter ion seemed to give longer-lasting seals. The pH was adjusted to 7.1 using 1 N KOH or CsOH. ATP and phosphocreatine were added to the IPS just before use to improve the metabolic state of the cells and to prevent activation of ATP-dependent currents.

Electrophysiological Measurements

After 22–28 hr incubation in medium 21212, cultures were washed 3–5 times in DBS at room temperature (22 ± 1°C). For patch-clamp measurements cell pairs were selected in which each cell had a diameter of 13–18 μm. Patch electrodes with tip resistances of 2–6 MΩ were fashioned from glass capillary tubes (Drummond Microcaps, 100 ml) and were coated with Sylgard® (Dow Corning, Midland, MI). Giga-seals were formed on both cells and the membrane patch at each electrode tip was ruptured to achieve the whole-cell clamp configuration. The electrodes were connected to a List Model EPC-7 or EPC-5 patch-clamp amplifier as described earlier (Veenstra & DeHaan, 1988). Records of voltages and currents filtered at 10 kHz were stored on VCR tape with a Neurocorder Model DR-484 digitizer (Neuro Data Instruments, New York, NY) in combination with a Panasonic Model NV-8950

Table 2. Conductance and frequency of occurrence of gap junction channels

Nominal γ_j (pS)	40	80	120	160	200	240
Expt. 021187						
Measured γ_j (pS)	51.3	87.8	126.9	162.4	202.3	249.5
SD	5.2	10.8	9.9	10.8	12.1	9.9
N (total = 73)	4	9	21	24	10	5
Expt. 040187						
Measured γ_j	—	78.8	129.0	152.6	—	238.9
SD	—	8.5	—	10.5	—	23.8
N (total = 173)	—	58	1	50	—	64
Expt. 081387						
Measured γ_j	50.2	82.3	121.9	154.9	196.9	258.0
SD	6.0	9.4	11.2	10.0	10.7	16.3
N (total = 95)	9	36	23	18	4	5
Expt. 120987						
Measured γ_j	45.8	—	—	—	—	—
SD	5.2	—	—	—	—	—
N (total = 36)	36	—	—	—	—	—
Expt. 121687A						
Measured γ_j	40.6	81.0	119.1	159.7	199.5	237.0
SD	8.0	7.8	7.8	9.2	9.1	11.1
N (total = 291)	78	55	36	66	43	13
Expt. 121687B						
Measured γ_j	41.5	80.3	116.7	155.8	193.7	251.0
SD	6.8	7.9	8.1	9.3	—	14.4
N (total = 289)	59	123	70	32	1	4
Expt. 012188						
Measured γ_j	45.5	81.4	120.5	160.9	201.4	235.1
SD	—	4.4	2.5	4.2	4.6	8.0
N (total = 96)	1	34	11	34	5	11
Expt. 020388B						
Measured γ_j	41.4	80.7	118.7	159.9	203.0	241.3
SD	1.8	3.0	1.8	2.0	5.3	5.7
N (total = 51)	6	6	8	7	15	9
Grand means						
Mean γ_j	42.6	80.7	119.6	157.7	200.4	240.3
SD	6.8	7.9	8.2	9.0	8.5	19.1
N (total = 1104)	193	321	170	231	78	111
% total	17.5	29.2	15.5	21.0	7.1	10.1

N = number of channel openings. The pipette solution for experiments 021187, 040187 and 081387 was IPS#57; G_j was 0.48, 0.80 and 1.65 nS, respectively. The pipette solution for experiments 120987, 121687A, 121687B, 012188 and 020388B was IPS#66; G_j was 0.08, 0.56, 0.38, 1.02 and 0.24 nS.

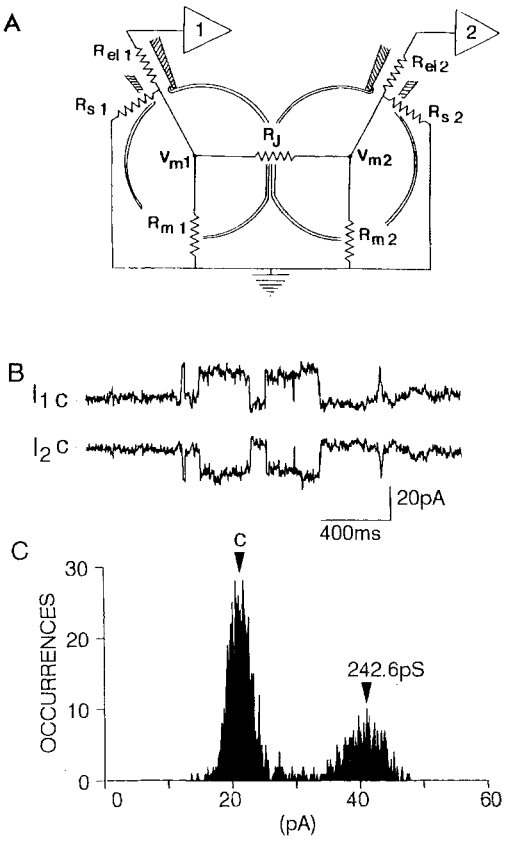

Fig. 1. Analysis of gap junction channel activity from a typical pair of 7-day chicken ventricle cells recorded during steady-state recording at 80-mV V_j. (*A*) The equivalent circuit of the two-electrode whole-cell patch clamp is shown after rupture of the membrane under the electrode tip. Each electrode has an access resistance to the cell interior (R_{el1}, R_{el2}) and a seal resistance (R_{s1}, R_{s2}) between the cell interior and the external reference. The membrane (input) resistance of each cell is R_{m1}, R_{m2}, while R_j is the junctional resistance between the cells. Membrane potential of each cell (V_{m1}, V_{m2}) is controlled separately by patch-clamp circuits represented by amplifiers 1 and 2. Typical values for the named resistances are R_{el} = 2–6 MΩ; R_s = 5–50 GΩ; R_m = 2–5 GΩ; R_j = 0.05–5 GΩ (G_j = $1/R_j$ = 0.2–20 nS). (*B*) A 2.5-sec segment taken from a 56-sec period during which V_1 was held constant at −10 mV and V_2 = −90 mV, yielding V_j = 80 mV. Because V_j is positive, opening channels allow outward current to flow from cell 1 (shown in I_1 as an upward deflection) across the junction into cell 2 (inward current shown in I_2 as a downward deflection). During the period of activity selected for this record the channel was open about 30% of the time. However, much of the rest of the 8.4 min of recording in this cell pair there were only sporadic openings with a total of 173 criterion events. (*C*) Amplitude histogram of the record shown. Mean conductance is 242.6 pS. Cell pair 040187, IPS#57.

VHS recorder and analyzed with a Nicolet 4094 digital storage oscilloscope interfaced with an IBM PC/AT computer. Current records were further low-pass filtered during playback with an Ithaco Model 4302 4-pole Bessel filter (Ithaca, NY) at 500 Hz for analysis of channel conductance levels and open times, or at 1 kHz for measurement of event transitions. Sample rates greater than twice the frequency of the analog filter bandwidth were used to reduce aliasing error.

Gap junction conductance was determined from the current response to transjunctional voltage steps ($G_j = I_j/V_j$). Unitary currents (i_j) through junctional channels were distinguished from peripheral membrane channel currents by the fact that in the whole-cell double patch-clamp configuration nonjunctional channel currents in either cell were recorded only in the electrode attached to that cell, while the current through gap junction channels was seen as symmetrical signals of equal size and opposite polarity in the two electrodes, i.e., as inward current in one cell and outward from its neighbor (Veenstra & DeHaan, 1988). Channel current amplitude was measured in two ways: by direct measurement of the current transitions from the oscilloscope

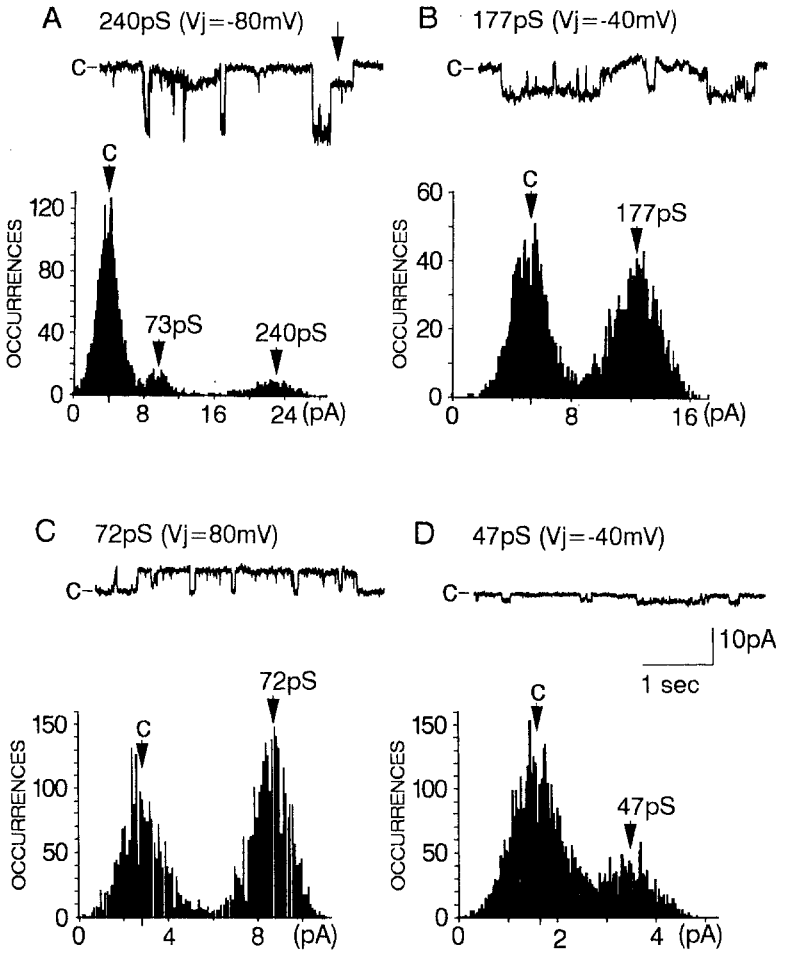

Fig. 2. Gap junction channel activity showing openings to four common conductance levels. The records are taken from different cell pairs. (*A*) Cell pair 121687A, −80-mV V_j, G_j = 0.56 nS, γ_j = 73 and 240 pS. (*B*) Cell pair 121687A, −40-mV V_j, G_j = 0.56 nS, and γ_j = 177 pS. (*C*) Cell pair 121687B, 80-mV V_j, G_j = 0.38 nS, and γ_j = 72 pS. (*D*) Cell pair 120987, −40-mV V_j, G_j = 0.08 nS, and γ_j = 47 pS.

screen and by computer-generated amplitude histograms. In junctions with G_j less than about 2 nS, baseline current was stable and background current noise was generally less than 2 pA (peak to peak). Steady-state records of this quality were analyzed by computer using the program MSINCH (Goolsby). MSINCH was designed to construct current-amplitude histograms and to calculate i_j from the interval between peaks. Cell pairs with higher conductance junctions often exhibited current drift and higher noise levels. Individual event transitions in these tracings could be distinguished as symmetrical signals in the simultaneous electrode records. Criteria for defining an event transition are given in the legend to Fig. 3. In these cases i_j was measured from such channel opening transitions directly from the oscilloscope screen. The duration of channel open times was also recorded. Unitary channel conductance (γ_j) was measured as i_j/V_j. Since the values of γ_j centered around multiples of 40 pS (*see* Table 2), we refer to the different channel sizes by their nominal conductance (40, 80 . . . 240 pS) in the text. For the present study we analyzed 3546 sec of data containing a total of 1104 channel openings from eight experiments.

To measure the voltage and time dependence of G_j, V_1 was held constant at −40 mV while the following sequence of 6-sec steps was applied to V_2: −40, −20, −40, −60, −40, 0, −40, −80, −40, 20, −40, −100, −40, 40, −40, −120, −40 mV, i.e., V_j (defined as $V_1 - V_2$) was stepped alternately to −20, 20, −40, 40 . . . . −80, 80 mV, with each step lasting 6 sec and separated from the last by 6 sec at V_j = 0 mV. At the beginning and end of each period of V_j = 0, a 100-msec pulse of V_m = −30 mV was applied to cell 2 to measure G_j with a noninactivating step of V_j = −10 mV. I_j was measured from the cell held at constant potential. The sampling interval for measuring peak I_j was 200 μsec/point.

Results

Embryonic Gap Junctions Have Channels with Multiple-Conductance Levels

To observe spontaneous steady-state channel activity, cell pairs were held at V_j = 80 or −80 mV with independent patch-clamp circuits (Fig. 1*A*) for repeated 56-sec recording periods. In cell pairs with low-to-moderate noise and little baseline drift (Fig. 1*B*), current-amplitude histograms (Fig. 1*C*) were produced by computer using the MSINCH program (*see* Materials and Methods). Figure 1*B* also illustrates the symmetrical signals of equal size and opposite polarity in the two electrodes that character-

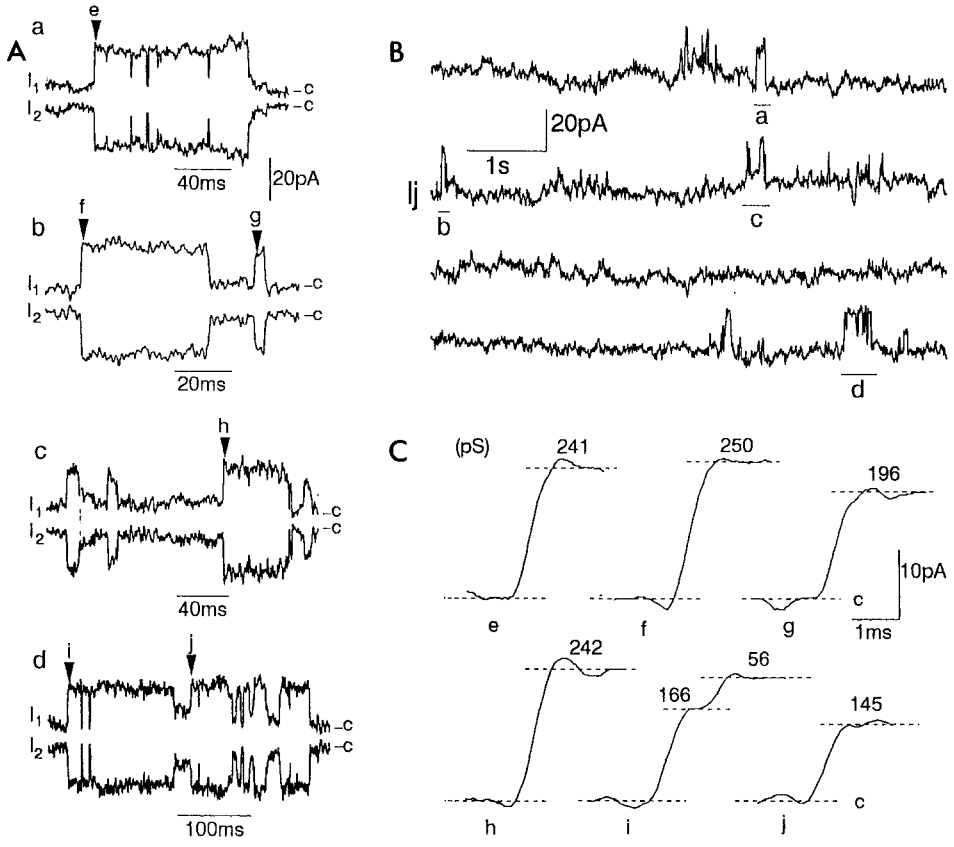

Fig. 3. Channel activity during steady-state recording at 80-mV V_j ($V_1 = -10$ mV, $V_2 = -90$ mV; $G_j = 0.80$ nS) shown at different time scales. (*A*) Records *a–d* illustrate typical channel activity, recorded simultaneously in both electrodes and displayed at time scales selected to show individual open-close events. Different conductance levels are evident especially in *b–d*. Data filtered at 1 kHz and displayed at 200 μsec/point. (*B*) The four tracings represent 30 sec of continuous recording (only I_1 shown) that include records *a–d* in *A*. (*C*) Each of the opening current transitions (labeled *e–j* in *A*) are displayed at fast sweep speed to demonstrate the direct method of measuring γ_j from the oscilloscope screen. Conductance levels were measured from these records (displayed at 50 μsec/point), using the following criteria. A stable i_j level was defined as at least 1 msec during which current fluctuated no more than ±1 pA around the mean. A transition was defined as a monotonically changing sequence of points to the next i_j level, which again had to have a dwell time of at least 1 msec. Five criterion openings (records *e–h* and *j*) are shown. Opening *i* is an example of a transition with a shoulder at 166 pS that would not be included in the data because the 166-pS level did not meet the 1-msec dwell-time criterion. Cell pair 040187, IPS#57.

ize gap junction channel openings (Veenstra & DeHaan, 1988; DeHaan et al., 1989). In these records, upward deflection represents outward current and downward shows inward current. The channel-amplitude histogram gives a mean i_j of 19.4 pA, measured between the baseline (closed) and open peaks. This represents a channel conductance of 243 pS. Dwell times at 80 and 160 pS could be seen in other records from this cell pair. Multiple values of γ_j were seen in most junctions studied. Analysis of records from eight junctions revealed six conductance levels with average values of 240.3, 200.4, 157.7, 119.6, 80.7 and 42.6 pS (Table 2) with frequent shifts from one to the other. Examples are shown in Fig. 2*A–D*. A shift from 240 to 73.5 pS is seen at the arrow in Fig. 2*A*. The mean conductance level of the openings in each of these records was obtained from amplitude histograms. During these steady-state recordings, periods of intense channel activity were interspersed with many seconds of little or no activity. The probability of channels opening at all, i.e., to any conductance level, was low, averaging less than about 20 openings/min. Even during the periods of greater activity, average fractional time in the open state was only 0.2–0.3.

Additional examples of large openings during such active periods are illustrated with dual traces in Fig. 3*A*,*a–d*. The sporadic nature of the activity is apparent from the 30-sec record that contains those periods (Fig. 3*B*), each of which is indicated by a bar lettered *a–d*. These events were selected to illustrate both the large openings and the method of channel

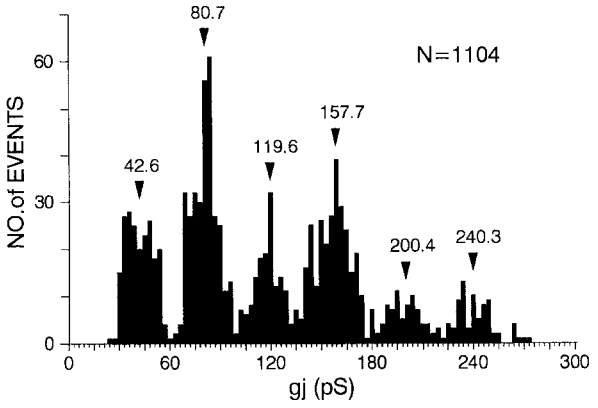

Fig. 4. Event conductance-level histogram. The conductances of each of the 1104 individual openings included in Table 2 were pooled and sorted as a histogram. The histogram shows six readily distinguishable peaks from 42.6 to 240.3 pS, with intermediate levels in approximately 40-pS increments.

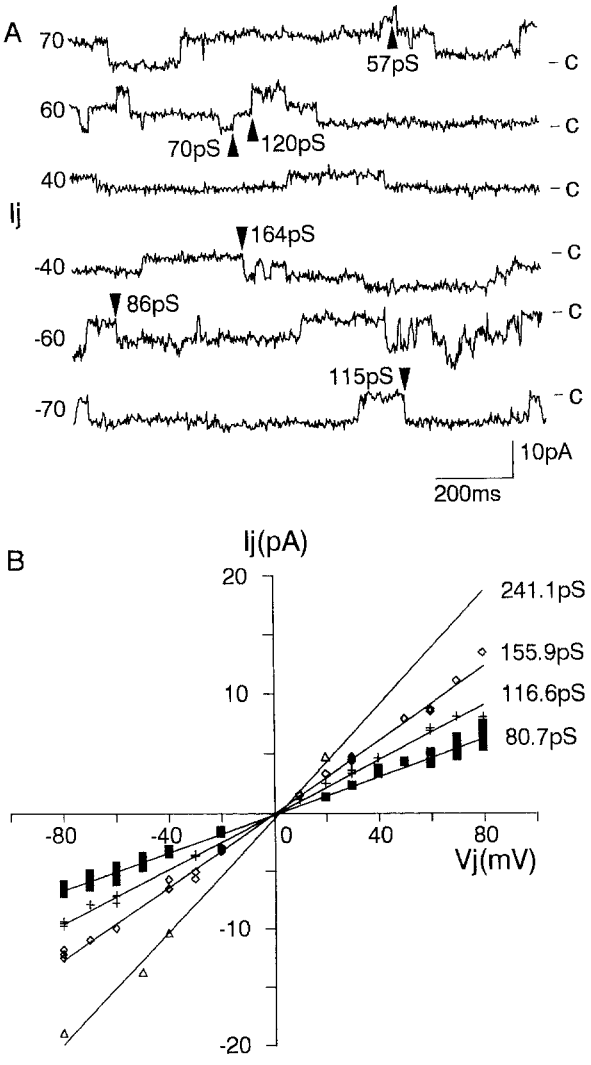

Fig. 5. Unitary channel currents as a function of V_j. (*A*) Sample records of I_j from a cell pair in which V_j was alternately stepped between positive and negative values between ±80 and ±10 mV in 10-mV increments for 2 sec each. V_j is shown at the left of each trace. Note that opening transitions are upward at positive potentials and downward when V_j is negative. (*B*) The *i/V* curves demonstrate that channel current increases linearly with V_j. Cell pair 121687B, IPS#66.

analysis directly off the oscilloscope. At fast sweep speed (Fig. 3*C*, records *e–h* and *j*) each opening current transition can be seen to meet the criterion of a smooth current shift between two stable levels (defined by a minimum of 1-msec dwell time at the closed and open levels). Openings with conductances of 145 to 250 pS are shown. The opening shown in Fig. 3*C*, record *i*, is an example that would be excluded from the data analyzed here because of the "shoulder" at 166 pS that has a dwell time less than 1 msec.

From direct measurements of 1104 channel openings in eight cell pairs, the conductance and frequency of occurrence at each conductance were averaged. The measured values and their standard deviations are shown for each conductance level in Table 2. To confirm that there was no arbitrary bias in determining the conductance categories, all 1104 openings were pooled and sorted into a channel conductance level histogram (Fig. 4). The six separate peaks confirm the modal nature of the conductance levels. Overall, the dominant channel types in these records were (nominally) 80 and 160 pS, together comprising approximately half the total events (Table 2). Openings at 40 and 120 pS were also common, while 200- and 240-pS openings were less frequent. The distribution among the different cell pairs varied widely. For example, activity in cell pair 040187 was distributed approximately equally among 80-, 160-, and 240-pS channels, with no openings to 40 or 200 pS evident. In contrast, in junction 120987 only 40-pS channels were active.

In experiments in which V_j was changed from −80 to 80 mV in 10-mV, 2- sec steps, i_j varied linearly with V_j and revealed discrete conductance levels (Fig. 5). Thus, unitary conductance was not voltage dependent.

Voltage Dependence of Gap Junction Conductance

As shown previously (Chen et al., 1988; DeHaan et al., 1989; Veenstra, 1990*c*) when potentials greater than ±20 mV are applied across the junction, I_j rapidly decays from its initial value (Fig. 6*A*). The resulting "spikes" of initial current (I_{init}, measured

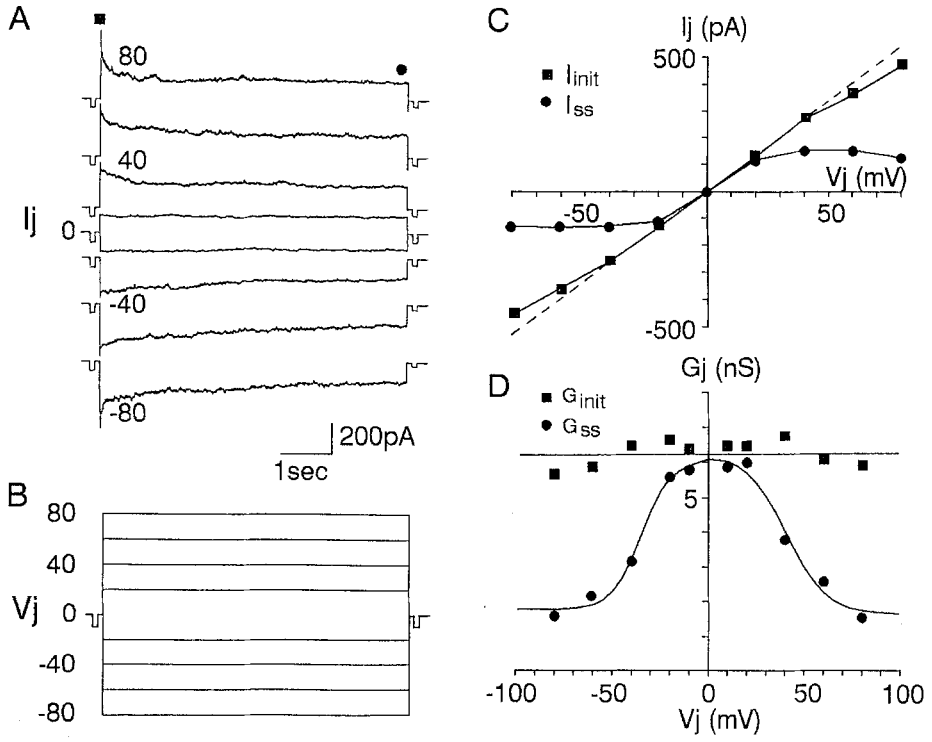

Fig. 6. Decay of gap junction currents. (*A*) Current traces ($I_j = I_1$) in response to the transjunctional voltage steps shown in *B* below. At all voltages, the initial current peak reflects the conductance of the junction just prior to the onset of the applied voltage. At values of V_j greater than ±20 mV the current decays over time to a lower steady-state value. (*B*) The membrane potential of cell 1 (V_1) was held constant at −40 mV while V_2 was stepped through a series of 6-sec alternating negative and positive pulses (−40 to −20, −60, 0, −80, 20, −100, 40, −120 mV to give ±20, ±40, ±60 and ±80 mV V_j). Each pulse was separated by a 6-sec period of V_j = 0 mV ($V_1 = V_2 = -40$ mV) to allow recovery. One hundred msec before the onset of each 6-sec voltage step a 10-mV, 100-msec test pulse was applied to measure the macroscopic junctional conductance (G_j) in the fully conducting state; a similar test pulse was introduced 100 msec after the end of each 6-sec step. (*C*) Initial (I_{init}) and steady-state (I_{ss}) junctional current from the records illustrated in *A* as a function of V_j. I_{init} (filled squares) is a linear function of V_j from −40 to 40 mV and deviates slightly at greater values of V_j. I_{ss} (filled circles) is nonlinear over the entire voltage range. The difference between the points at each V_j represents the voltage-dependent decay of I_j. The amount of current decay increases with V_j between ±20 and ±80 mV. (*D*) Junctional conductance (G_{init} and G_{ss}) as a function of V_j. From −80 to 80 mV V_j G_{init} deviates slightly from linearity while G_{ss} shows a much steeper dependence on V_j and yields the familiar bell-shaped Boltzmann relationship. The data for G_{ss} are fit by curves produced from the Boltzmann equation (*see* text). For the steady-state conductance A = 0.037, and V_0 = ±39 mV. Cell pair 020388, IPS#66.

200 μsec after the start of voltage step) are most prominent at ±60 and ±80 mV. Resting G_j (near 0 V_j) could be measured without perturbation by applying a brief 10-mV test pulse of V_j. Figure 6 illustrates an experiment utilizing this technique designed to determine the junctional current-voltage relationship. The membrane potential of cell 1 (V_1) is held constant at −40 mV while V_2 is stepped from −40 to −20 mV (V_j = −20 mV) for 6 sec before returning to −40 mV (V_j = 0 mV). After 6 sec at 0 V_j to allow complete recovery, V_2 is stepped to −60 mV for a 6-sec pulse of V_j = 20 mV. As shown in Fig. 6*B*, this pattern was then repeated with alternating pulses of V_j preceded and followed by 10-mV test pulses. The test pulse at the end of the 0 V_j period measures the fully recovered conductance G_{rec}. Averaging these currents from six repeated steps in this cell pair gave G_{rec} = 6.4 ± 0.38 nS. Measuring I_{init}/V_j immediately after the onset of each large voltage step in the above series yielded G_{init} = 6.35 ± 0.38 nS, indicating that the initial current response to a step from 0 V_j is a measure of the resting conductance of the junction just prior to the application of the pulse. In five experiments, mean G_{init}/G_{rec} = 0.93 ± 0.07 (n = 30). The flat current records in Fig. 6*A* at 20 and −20 mV confirm that no time-dependent change in current is observed at those levels. Among the 31 cell pairs in the present study, G_j ranged from 0.24 to 22.5 nS. Data used for this study was obtained from 12 of these in which G_j was less than 7 nS.

Since I_j (= I_1) is measured from the cell whose potential remains constant during application of the

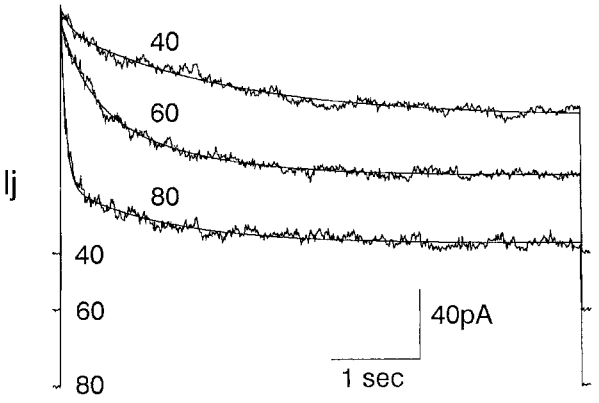

Fig. 7. Rate of current decline varies with V_j. I_j averaged from seven pulses each to V_j = 40, 60, and 80 mV. The 40- and 60-mV responses are shifted so their peaks correspond to that of the 80-mV curve. The averaged currents are fit with biexponential functions with the following values of τ_1 and τ_2: 40 mV, 112.4 msec and 1.9 sec; 60 mV, 294.1 msec and 1.1 sec; 80 mV, 56.7 msec and 1.2 sec. The response to the 80-mV pulse could also be fit with a triexponential curve with equal goodness-of-fit parameters. Cell pair 121390, IPS#57. The time constants and the ratio G_{ss}/G_{init} averaged from five such experiments are shown in Table 4.

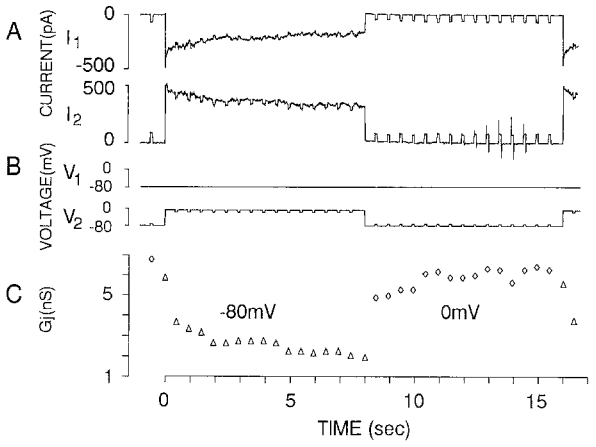

Fig. 8. Decline and recovery of macroscopic junctional conductance. (*A*) I_1 and I_2 in response to the voltage protocol shown in *B*. The steady-state resting conductance (V_j = 0 mV) is tested with a 10-mV pulse before application of a larger potential (time 0) designed to produce a decay in G_j. At 8 sec, V_j is returned to 0 mV and conductance continues to be probed every 400 msec with a 10-mV test pulse. (*B*) V_1 was held constant at −80 mV while V_2 was alternated in 8-sec steps between −80 mV (V_j = 0 mV) and 0 mV (V_j = −80 mV). Superimposed on the 8-sec steps were 10-mV, 100-msec test pulses every 400 msec to measure the conductance without causing additional effects on G_j. (*C*) Change in G_j during the decline and recovery phases. Just prior to time 0 (onset of step to −80 mV V_j) the conductance measured with the last 10-mV test pulse at 0 V_j (◇) is 6.8 nS. The first conductance measurement at −80 mV, 200 μsec after the voltage step, (△) is 5.9 nS. This conductance rapidly declines to 2.5 nS in less than 1 sec and continues to decay more slowly to 1 nS over the remaining 7 sec. After the return to 0 V_j, (◇) the initial recovery of conductance is rapid (G_j = 5 nS within 500 msec), after which G_j gradually returns to 6–7 nS by the end of the 8-sec period. The rate constants for the biexponential recovery, averaged from four such sequences were 43.9 msec and 2.3 sec, respectively. Cell pair 020388, IPS#66.

step in V_j, there is no contamination of the records by nonjunctional currents or passive membrane time dependencies. This assures that the decay of the current in the first few seconds reflects solely a reduction in G_j. The I_{init}/V_j curve (Fig. 6*C*) approximates a straight line with a slope conductance of 6.4 nS. However, at $V_j = \pm 60$ and ±80 mV, I_{init} deviates slightly from linearity. For the preparation illustrated in Fig. 6, the deviation is 19% at −80 mV and 16% at 80 mV. From five experiments the mean deviation at −80 mV was 14% and at 80 mV it was 16%. These values are not appreciably different when measured 100 or even 50 μsec after the onset of the pulse, suggesting that the mechanism of this "instantaneous" deviation from linearity is different from the time-dependent decline.

In contrast to I_{init}, I_{ss} becomes clearly nonlinear at voltages beyond ±20 mV. The larger the V_j, the greater the magnitude and faster is the current decline (Figs. 6*A* and 7). The relationship of conductance change to V_j is shown in Fig. 6*D*. We found that steady-state conductance could be fit with a Boltzmann equation of the following form:

$$G_j = [(G_{max} - G_{min})/\{1 + \exp A(V_j - V_0)\}] + G_{min}$$

where A is a constant expressing the voltage sensitivity of the gap junction channels and V_0 is the transjunctional voltage at which the conductance is half-maximal (Fig. 6*D*). From five experiments, residual conductance (G_{ss}/G_{init}) was 0.36 ± 0.12 at V_j = −80 mV and 0.37 ± 0.11 at 80 mV (n = 20). The fractional conductances at those potentials (G_{80}/G_{max}, G_{-80}/G_{max}) predicted by the Boltzmann relation were, respectively, 0.31 and 0.30. The extrapolated theoretical values of G_{min}/G_{max} were 0.27 in both polarities, as shown with the other parameters from the Boltzmann fits in Table 3. The observed residual conductances are larger than those predicted by the Boltzmann relation at ±80 mV because G_{init} was consistently about 15% smaller than the fitted G_{max}. This resulted from the instantaneous deviation from linearity described above.

Kinetics of Conductance Decay and Recovery

The kinetics of the decline in junctional conductance as well as its magnitude varied with V_j. A typical experiment showing I_j in response to 40-, 60-, and

Table 3. Voltage-dependent parameters of junctional conductance[a]

V_j	n	G_{max} (nS)	G_{min} (nS)	G_{min}/G_{max}	V_0 (mV)	A
Negative	20	4.54 ± 0.81	1.22 ± 0.28	0.27	−42.72 ± 3.36	0.06 ± 0.12
Positive	20	4.67 ± 0.58	1.29 ± 0.30	0.27	42.56 ± 2.95	0.13 ± 0.14

[a] Pooled data of the type illustrated in Fig. 6*D* from five experiments fit with a Boltzmann equation of the form: $G_j = [(G_{max} - G_{min})/\{1 + \exp A(V_j - V_0)\}] + G_{min}$, where G_{min} is the theoretical conductance extrapolated to infinite voltage, V_0 is the transjunctional voltage at which the conductance is half-maximal, and A is a parameter expressing the voltage sensitivity of the gap junction channels.

Table 4. Kinetics of voltage-dependent decay and recovery of junctional conductance[a]

V_j (mV)	τ_1 (msec)	n	τ_2 (sec)	n	G_{ss}/G_{init}
			Decay		
−80	126.0 ± 13.9	20	2.09 ± 0.15	20	0.36 ± 0.12
−60	185.6 ± 14.5	20	2.66 ± 0.21	20	0.46 ± 0.21
−40	757.3 ± 345.3	20	4.31 ± 2.21	12	0.66 ± 0.22
40	399.5 ± 19.4	20	2.92 ± 0.43	9	0.66 ± 0.15
60	309.2 ± 23.8	20	3.36 ± 3.32	20	0.46 ± 0.16
80	127.3 ± 45.8	20	2.59 ± 1.24	20	0.37 ± 0.11
			Recovery		
−80	327.9 ± 36.7	30	2.25 ± 0.43	30	
80	225.2 ± 29.1	30	1.87 ± 0.30	30	

[a] Data pooled from five experiments of the type illustrated in Figs. 6 and 8, showing means, SDS, and number of averaged current records.

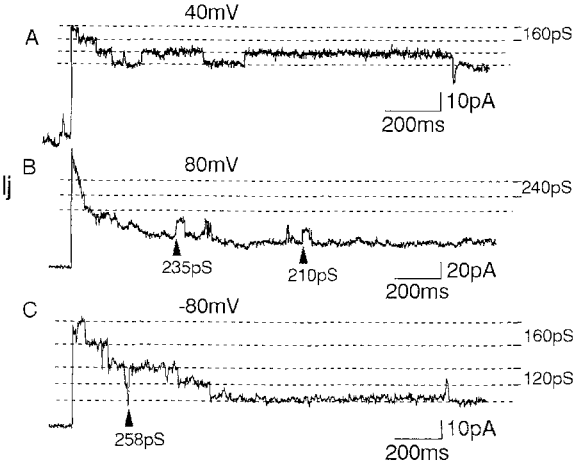

Fig. 9. Stepwise current decay in low conductance junctions. (*A*) In a cell pair with resting G_j = 0.75 nS, application of a step directly from −40 to 40 mV V_j results in an initial peak current of 61 pA followed by a decline in discrete steps of 160 pS. Cell pair 021187, IPS#57. (*B*) Response to a 5-sec pulse from V_j 0 to V_j 80 mV in a cell pair with a junction in which resting G_j averaged 2.1 nS. Current decay is associated mainly with closure of 240-pS channels that occasionally reopen. A clear 210-pS event is also evident. The sloping initial decay corresponds to poorly resolved 40–80 pS channel closures. Cell pair 011388, IPS#66. (*C*) Current decay seems to result mainly from 160- and 120-pS channel closings. This record has been inverted for this illustration. Cell pair 121687B, IPS#66.

80-mV steps in V_j is illustrated in Fig. 7. The decay time constants and the ratio G_{ss}/G_{init} pooled from five such experiments are summarized in Table 4. At ±80 mV the current decays sharply at first with a fast time constant (τ_1) of 50–150 msec. As decay continues, at least one slower process is revealed with a longer time constant (τ_2) on the order of 2–4 sec. In a few cases, the ±80-mV current could be fit with a triexponential function, with the third time constant on the order of tens of seconds. On average, the time constants become progressively slower at ±60 and ±40 mV (Table 4).

The recovery of G_j after the return of V_j to 0 mV was measured by the voltage sequence illustrated in Fig. 8*B*. In these experiments V_1 was held constant at −80 mV while V_2 was alternated between −80 mV (V_j = 0 mV) and 0 mV (V_j = −80 mV) every 8 sec. Superimposed on these large square pulses, 100 msec, 10-mV test pulses were applied to measure instantaneous G_j at intervals of 400 msec continuously. The conductance recovery upon return from 80 to 0 mV V_j (averaged from six voltage sequences each in five experiments) was best fit by a double exponential with τ_1 = 225 msec and τ_2 = 1.9 sec (Table 4).

Conductance Decline Reflects Changes in Channel Conductance Levels

In junctions with few active channels and low G_j, voltage-induced conductance decline does not follow a smooth exponential decay curve but occurs in discrete steps. In the record from the cell pair depicted in Fig. 9*A* a series of 160-pS conductance levels are defined by dotted lines. The current decay in this junction during the initial 2 sec after the voltage step clearly results from the sequential closing of three 160-pS channels. The record shown in Fig. 9*A* was in response to an 80-mV step in V_j (from −40 to 40 mV) applied early in the experiment. At that time, G_j was about 0.75 nS. Later in the

experiment, presumably as a result of the effects of the high intracellular calcium from IPS#57 (Veenstra & DeHaan, 1988), G_j fell to 0.48 nS, which is the value given for this preparation (#021187) in Table 2, at the time unitary channel activity was recorded. Figure 9*B* (#011388) and Fig. 9*C* (#121687B) show the more usual pattern of conductance decay which does not normally result from closure of a single channel type. In these records, closure and occasional reopenings of 240-, 200-, 160- and 120-pS conductance levels are evident in apparently random sequence during the course of the conductance decay.

Does a 160- or 240-pS conductance level represent the simultaneous opening, respectively, of four or six randomly fluctuating 40-pS subunit channels? The frequent appearance of rapid shifts between conductance levels as illustrated here (Figs. 2*A*, 3*C* and 5*A*) without intervening 40-pS increments argues strongly against such a model. Occasional particularly favorable cell pairs with junctional conductance so low that it appears that only a single channel is active provide additional evidence against this model. In Fig. 10*A* current records are presented from a cell pair in which a single 242-pS channel and an occasional 40-pS channel are active in the resting junction. Using the voltage sequence of Fig. 8*B*, each current trace shows I_j in response to a 10-mV test pulse at the end of an 8-sec rest period at 0 V_j, followed 400 msec later by the response to a step to 80 mV V_j (Fig. 10*A*) or −80 mV V_j (Fig. 10*B*). The mean current generated by the 10-mV test pulses is 2.42 ± 0.039 pA, indicating that during most of the recovery period a single 242-pS channel was consistently open. The steps to 80-mV V_j produce an instantaneous current through the open channel in each record which is approximately eight times larger than the 10-mV pulses (18.4 ± 2.3 pA; mean G_j = 230 pS). This voltage step is followed shortly by partial or complete channel closure (Fig. 10*A* and *B*). In Fig. 10*A*, record *a*, for example, the channel remains open for 16 msec after onset of the 80-mV V_j, closes down to 77 pS for 10 msec, then reopens to 240 pS for 80 msec, and finally closes completely. In record *b*, the channel remains open with some flickering for 230 msec and then closes to a 42.4-pS state. Between V_j steps in the opposite polarity (Fig. 10*B*), the channel is open to a small substate during some of the 10-mV test pulses (records *c* and *f*). After stepping to −80 mV, the channel is seen to be closed during a few sweeps (record *c*) or is open to 40 pS (record *f*). However, the open channel tends to stay open longer than it does with positive steps, or it reopens several times during the first few hundred msec (Fig. 10*B*, record *b* and *d*). This behavior is reflected in the ensemble averages of the records (record *i*), which roughly mimic the current decay seen in the higher conductance junctions (Figs. 6*A* and 7). Three biphasic sequences of decay and recovery of G_j in this junction are shown in Fig. 10*C* and *D*. The responses to each of 15 10-mV test pulses applied during the recovery period at V_j 0 revealed that the single 240-pS channel was open during the entire 8-sec interval (Fig. 10*C*). Responses to −10-mV pulses following 8 sec at −80 mV were not so uniform (Fig. 10*D*); 40% of these test pulses revealed a 120-pS substate. Nonetheless, this experiment indicates that the fully open channel at V_j near 0 has a conductance of about 240 pS, while the channel closes or shifts to lower conductance states upon application of V_j = ±80 mV.

Additional evidence that large channel openings are replaced by lower conductance levels in response to application of a large step in V_j is shown in Fig. 11, in which junctional currents in response to 5-sec pulses to −80 mV V_j (Fig. 11*A*, records *a–f*) are shown for a 0.56-nS junction. The ensemble average of 16 such records (Fig. 11*A*, *g*) mimics the current decline in high conductance junctions and can be fit by a biexponential function. Here, amplitude histograms of channel activity during the initial 1.1 sec after onset of a step in V_j, are compared with those taken during the final 1.1 sec of the step, when conductance decay is complete. Simple inspection of the records indicates that early in the voltage pulse a range of large conductance channels is active. This is corroborated by the amplitude histogram of the initial 1.1 sec (Fig. 11*B*) which reveals a maximal unitary channel conductance level at 234 pS with a small shoulder at 80 pS buried in the noise. In contrast, during the final 1.1 sec of the voltage pulse (Fig. 11*C*) the small level near 40 pS predominates.

Discussion

Although gap junctions were recognized over a quarter of a century ago as the site of electrical coupling among heart cells (reviewed in DeHaan et al., 1981; Loewenstein, 1981; Page & Manjunath, 1986), it is only in the last few years that we have begun to understand their molecular composition and functional properties (Beyer, Paul & Goodenough, 1990; Spray & Burt, 1990; Bennett et al., 1991). These structures consist of cylindrical arrays of integral membrane protein complexes that form hemichannels or connexons (Goodenough, 1976) which, by alignment with their counterparts in adjacent cells, establish channels that connect the two cytosolic compartments. Each connexon is a hexamer of six rod-like subunits composed of one of a multi-gene

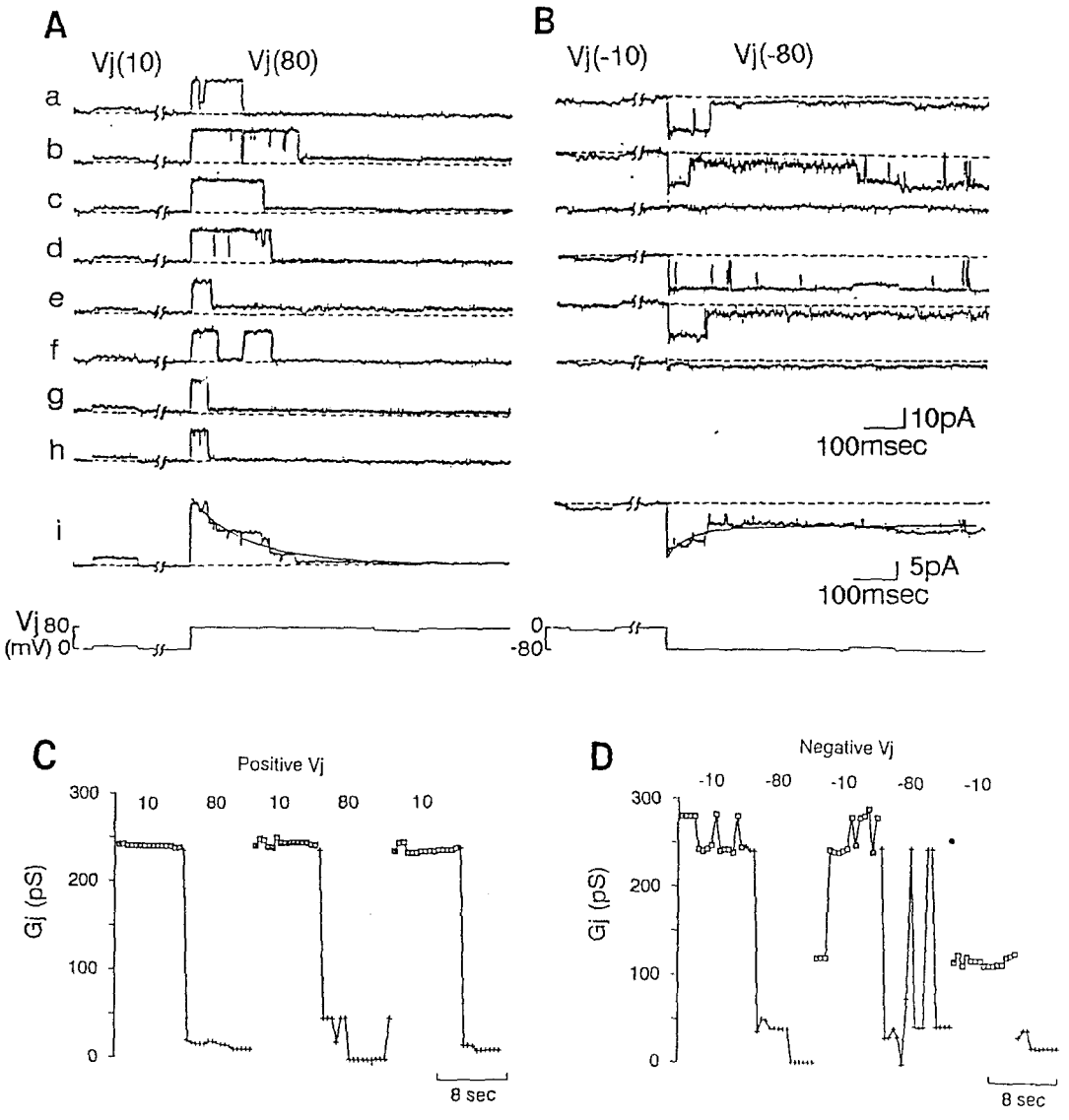

Fig. 10. Channel activity in a very low conductance junction. (*A*) Eight records (*a–h*) of I_j in response to repeated steps in V_j to 80 mV. (*B*) Six steps to −80 mV separated by 8 sec of V_j 0. Superimposed on the large voltage steps were 10-mV, 100-msec test pulses applied every 400 msec throughout the sequence, as shown in Fig. 8. Each trace is preceded by the current response to the last 10-mV test pulse at the end of the 8-sec recovery period at 0 V_j. The ensemble averages of the individual records (*i*) are best fit with biexponential curves with time constants for positive V_j of τ_1 = 114.4 msec and τ_2 = 14.3 sec and for negative V_j of τ_1 = 42.2 msec, and τ_2 = 1.0 sec. (*C*) G_j calculated during three consecutive 8-sec cycles of 80 mV V_j and 0 V_j tested with 10-mV pulses. The conductance during each recovery period at 0 V_j is indicated with open square symbols (periods marked 10); during application of 80 mV, G_j measurements are indicated with + symbols. Every test pulse at 10 mV reveals a single fully open 240-pS channel. (*D*) Same as *C*, but measured at −10 and −80 mV. At V_j = −10 mV, most pulses also reveal a single 240-pS channel but a few measure 280 pS, indicating the activity of a second superimposed 40-pS conductance. During the recovery phase of the third cycle the −10-mV test pulses show the 240-pS channel in a half-open state at 120 pS. Cell pair 021388, IPS#66.

family of channel-forming proteins, termed connexins. Cardiac gap junctions contain primarily a 43-kD polypeptide, connexin43 (Beyer et al., 1990). A structural model of the connexin monomer predicts that the connexin polypeptide configuration has four transmembrane-spanning regions. The amino- and carboxy-termini and a loop between the second and third membrane-spanning domains are located on the cytoplasmic side of the membrane (Beyer et al., 1990; Bennett et al., 1991). The amino-terminus and the extracellular and transmembrane domains are all highly conserved among the connexins, while the

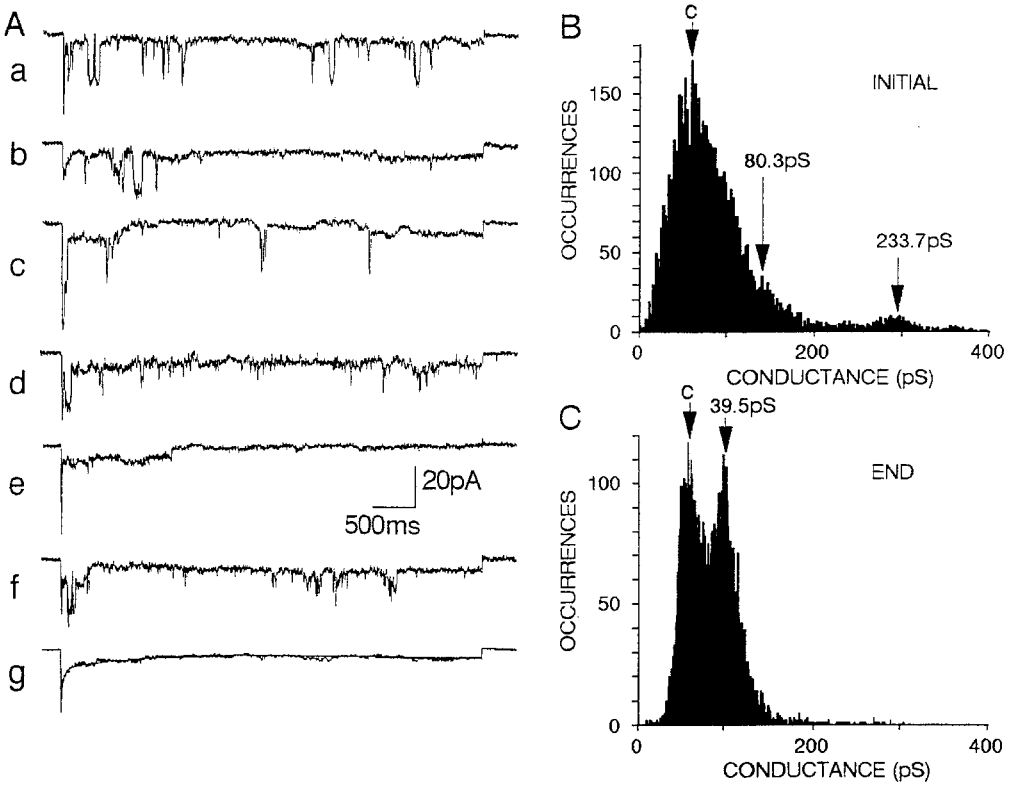

Fig. 11. (*A*) *a–f*. Current responses to six 5-sec steps to −80 mV V_j in a junction with a mean resting conductance of 0.56 nS. *g*. The ensemble average of 16 such records is fit with a biexponential curve with $\tau_1 = 25.3$ msec and $\tau_2 = 559$ msec. (*B*) Amplitude histogram of channel activity during the initial 1.1 sec of each of the individual records, showing a maximal conductance level of 234 pS and smaller levels buried in the noise surrounding the closed state. (*C*) Amplitude histogram of channel activity during the final 1.1 sec of each of the individual records reveals a single major conductance level of 39.5 pS. The noise is lower in this case because the larger conductance levels are suppressed at the end of the pulse. Zero conductance on the abscissa in *B* and *C* represents 0 amplifier current. Cell pair 121687A, IPS#66.

central loop and carboxy-terminal tail vary greatly in both sequence and length. The amino acid sequences of the four membrane-spanning domains (M1–M4) are largely nonpolar except for M3. This region is thought to form an amphipathic helix with the polar portion constituting part of the wall of the aqueous pore. Nonetheless, all four of these domains differ greatly from those of the Na^+, K^+, and dihydropyridine-sensitive Ca^{2+} channels (Catterall, 1988; Jan & Jan, 1989). These nonjunctional voltage-sensitive channels contain a sequence in which an arginine or lysine is present at every third position, interspersed with more hydrophobic residues. This transmembrane "S4 sequence" is believed to function as the voltage sensor. None of the connexins exhibit an S4 sequence (Jan & Jan, 1989; Spray & Burt, 1990). However, it has been suggested that a voltage sensor may reside in the carboxy-terminal tail or the central loop of some connexins (Spray et al., 1990).

Chick Heart Junctional Channels Have Multiple Conductances

We have shown that junctional channel events in embryonic cardiac cell pairs occurred mainly during spontaneous periods of intense activity separated by long periods of rare openings. Most junctions showed multiple conductances (Table 2, Figs. 2 and 3). Confirming previous reports (DeHaan, 1988; Veenstra & DeHaan, 1988; DeHaan et al., 1989; Veenstra, 1990*c*) the dominant open states in these junctions are near 80 and 160 pS. From measurements in eight low conductance cell pairs, we found more than 50% of 1104 discrete events at these two conductance levels (Table 2). But the frequencies of openings to the 40- and 120-pS states were almost as great, and 10% of the events were 240 pS. Overall, 200-pS openings were least common. However, the distribution of channel sizes varied substantially among different cell pairs. Although the nominal

240-pS state was present as the maximal uninterrupted current transition in all but one experiment (#120987, Table 2), small openings were favored in some junctions (e.g., #081387 and 121687B) while others exhibited a greater frequency of large channel events (040187, 012188 and 020388B). Openings to 200 pS were absent or rare in five of the experiments listed in Table 2 but constituted almost one-third of the events in cell pair 020388B.

Our finding of several conductance levels cannot be ascribed to a single population of uncoordinated, stochastically active 40–50 pS channels. Such a model can be ruled out by the observed characteristics of the openings and the statistics of their occurrence (Läuger, 1985; Fox, 1987). If openings to levels between 80 and 240 pS resulted from the random simultaneous superposition of two to six 40-pS channels, the frequency of appearance of the progressively larger conductances should approximate an inverse power series, with the likelihood of appearance of the 240-pS level becoming vanishingly small. Furthermore, random superposition would only rarely result in smooth transitions to a large conductance level, whereas we commonly observe such transitions (Fig. 3). The data are consistent, however, with three other possible models: (i) 40-pS channels that exhibit cooperativity; (ii) 240-pS channels with substates; or (iii) channels of different sizes.

The cooperating channels of model 1 are envisioned as two-state devices that can be either closed or fully open to a homogeneous pore size that yields a conductance of 40 pS. Versions of model 1 would include the "multiport" proposed by Hunter and Giebisch (1987) to explain the behavior of renal tubular K channels or the "minipores" that are proposed to form the cooperatively gated units of porin (Schindler, 1989). At present, no ultrastructural or molecular evidence of a mechanism for such cooperative behavior among groups of connexons is available (*see* discussion in Chen & DeHaan, 1992).

Model 2 imagines a channel that can exist in several different configurations, each with a different conductance. Measurements of unit channel conductance from a variety of nonjunctional voltage-gated and ligand-gated channels reveal that some (perhaps most) channels can exhibit more than a single open-state configuration. Examples include SR K channels (Fox, 1987; Hill, Coronado & Strauss, 1990), neuronal glutamate-activated channels (Jahr & Stevens, 1987), sodium channels (Patlak, 1991), and the cardiac inward rectifier (Sakmann & Trube, 1984; Kell & DeFelice, 1988). Strong evidence for the concept of substates in embryonic cardiac gap junction channels is provided by single-channel activity of the kind illustrated here in Fig. 10. In the fortunate case of a junction that apparently contained only one or two active channels, one was found to be open to its maximal conductance all 45 times it was probed with a 10-mV test pulse during three 8-sec periods of 0 V_j (Fig. 10*C*) and 71% of the times it was tested with a −10-mV pulse. This indicates that with no applied V_j, under the conditions represented, the main open state of the channel was near 240 pS, and that the probability of its being open to that conductance level must have been near unity most of the time. Within 200–300 msec after application of $V_j \pm 80$ mV, openings were limited almost entirely to 80 pS or less. Other gap junction preparations suitable for measuring γ_j have also revealed multiple conductances. Channels measured in pairs of mouse pancreatic acinar cells had discrete γ_j levels of 27 and 130 pS, and in Chinese Hamster ovary cell junctions in which G_j was reduced by carbachol or OAG (a derivative of diacyl-glycerol) five reproducible levels were reported between 22 and 120 pS (Somogyi & Kolb, 1988; Kolb & Somogyi, 1990). Moreover, in many reports that feature a single dominant value of γ_j, smaller events are pictured in the recordings or are identified as potential subconductance states (e.g., Young, Cohn & Gilula, 1987; Burt & Spray, 1988; Eghbali, Kessler & Spray, 1990; Moreno et al., 1991).

Substates could be expected from certain interpretations of ion channel models that visualize closure as resulting from a helical twisting (Catterall, 1988; Millhauser, 1990) or tilting (Unwin, 1989) of the pore-forming subunits. In the open state, a polar region of an amphipathic transmembrane helix is thought to line the wall of the aqueous pore. The twisting motion of the subunits could move nonpolar groups into the channel, thereby occluding it. Bennett et al. (1991) have elaborated such a model for the connexon. One way to explain our six equally spaced conductance levels is to postulate that the fully open 240-pS channel has each of its six connexin subunits free to twist independently of the other five. If rotation of each connexin subunit were to occlude one-sixth of the cross-sectional area of the channel pore, the result would be a channel with six conductance substates at 40-pS increments. We have discussed the substate model in detail elsewhere (Chen & DeHaan, 1992).

Channels of different sizes (model 3) might result from isohexamers of different connexins as suggested by Swenson et al. (1989), from pairing of heterologous connexons (Rook et al., 1989; Swenson et al., 1989; Werner et al., 1989), or from heterohexamers composed of different combinations of connexins. There is mounting evidence that channels formed from different members of the connexin family (Beyer et al., 1990) have different conduc-

tances. Beyer (1990) has found three connexin isoforms in the chick embryo, Cx42, Cx43 and Cx45. In a wide variety of preparations in which Cx43 predominates as the gap junction protein, γ_j is in the narrow range of 40–60 pS (Burt & Spray, 1988; Rook et al., 1988; Rudisuli & Weingart, 1990; Veenstra, 1990*a*; Giaume et al., 1991). Consistent with this result are the recent preliminary findings of Veenstra et al. (1991). With pairs of communication-deficient mouse N2A cells stably transfected with constructs containing cDNA of Cx43, these workers found channels with γ_j of about 50 pS. In contrast, similar cell pairs caused to express Cx42 or Cx45 had unitary conductances of 150 or 30 pS, respectively. Comparable results with the hepatic connexins have been reported. The main conductance of gap junction channels formed from Cx32 expressed in transfected SKHep1 cells was about 150 pS (Eghbali et al., 1990), whereas when hepatocyte membranes containing gap junction channels composed of Cx26 and Cx32 were incorporated into lipid bilayers, two levels of γ_j were evident at about 150 and 80 pS (Moreno et al., 1991, corrected for $[K^+]$).

Varied conductances can also result from different flicker rates in a channel (Yellen, 1984; Hill et al., 1990). However, Patlak (1991) has noted that this mechanism would predict that intermediate conductance states would be noisier than either the closed or fully open state. On these grounds he discounts flicker rate as an explanation for substates in sodium channels. Earlier experiments with embryonic chick cardiac cell pairs in which channel activity was recorded at 22-kHz sampling frequency and displayed after low-pass filtering at bandwidths of 1–10 kHz revealed little flickering and no appreciable changes in measured channel conductance (Veenstra & DeHaan, 1988, Fig. 4), as would have been predicted if flickering were in the millisecond or kilohertz range (Millhauser, 1990).

Is Pore Size Constant at Different G_j?

One way to distinguish a homogeneous population of small, cooperative channels (model 1) from either of the alternative models that postulate the existence of large, high conductance channels, would be to measure pore size directly by diffusion of marker molecules of known dimensions. The effective diameter of junctional channel pores was reported to change under the influence of agents that alter G_j (reviewed in Loewenstein, 1981). For example, Schwarzmann et al. (1981) used a series of linear uncharged fluorescently labeled glycopeptides of progressively increasing molecular diameter as probes in cultured mammalian cells. With junctions maintained under conditions that promoted high conductance, the cut-off size for tracer passage was about 1.6 nm, similar to the size found in pairs of mammalian ventricular cells (Imanaga, Kameyama & Irisawa, 1987). Elevation of intracellular calcium caused concomitant decreases in G_j and in cut-off size, suggesting a constriction in mean diameter of the channel pores. In contrast, Zimmerman and Rose (1985) coinjected pairs of tracers of different size and fluorscence wavelength into *Chironomus* salivary gland cells and measured the rate constant of diffusion for each dye into a neighboring cell. Under conditions that modified overall junctional conductance by more than sevenfold, the permeability ratio for large and small molecules in these preparations remained constant, suggesting that differences in G_j resulted from regulation of the number of open channels at any instant, not the channel pore size or selectivity. Similarly, in pairs of amphibian blastomeres Verselis et al. (1986) demonstrated that junctional permeability (P_j) and G_j were linearly related over a wide range of G_j values. This result is consistent with the idea that junctional channels are two-state devices with no intermediate conductances. Similar dye-diffusion experiments have not been done with embryonic heart cells.

We reported earlier that the predominant junctional channel conductance in chick cardiac myocytes was 166 ± 51 pS (Veenstra & DeHaan, 1988). From independent data sets, Veenstra (1990*a*,*c*) found that mean γ_j was 166 ± 37 pS and we report here a value of 158 ± 9 pS (Table 2). This nominal 160-pS conductance level was prominent in all but one of the preparations pooled in Table 2. Openings at this conductance level were found over the entire range of V_j values tested (−80 to 80 mV), in the face of wide disparities of intracellular $[Ca^{2+}]$, and in preparations spanning wide differences in G_j. This finding is corroborated here by the observation (Fig. 5) that i_j is linear and γ_j is unaffected by V_j from −80 to 80 mV. The early result initially led us to the interpretation that if both γ_j and N in the relation $G_j = \gamma_j N P_o$ remained constant with G_j, changes in G_j must be explainable entirely on the basis of P_o (Veenstra & DeHaan, 1988). However, it seems from the present data that agents that alter G_j also change the frequency of occurrence of the various conductance levels. This is shown for the effect of V_j in Fig. 11. Here, large openings that are prevalent during the initial phase of a −80-mV pulse of V_j are largely suppressed in favor of 40-pS openings at the end of the pulse. The effects of octanol (Veenstra & DeHaan, 1988) can be interpreted similarly as limiting channels from opening to their largest con-

figurations. Thus agents that reduce G_j in embryonic gap junctions may do so as a result of two effects: reducing P_o; and shifting from large conductance states to small, thereby decreasing average pore size. In a dye-diffusion experiment this would result in a retardation of large tracer molecules.

Voltage Dependence of Cardiac Gap Junctions

It is well-documented that cell-to-cell conductance between adult cardiac myocytes is insensitive to the potential across the junctions (e.g., Noma & Tsuboi, 1987). In contrast, voltage-regulated gap junctions are common in embryonic tissues (Spray et al., 1981; DeHaan et al., 1989; Ebihara et al., 1989; Spray et al., 1990). The experiments pictured in Figs. 6–11 confirm that chick cardiac gap junctions are in a high conductance state at rest (near 0 V_j). When a large potential (e.g., ±80 mV) is applied across the junction, G_j declines along a biexponential time course to less than one-third its original value. As noted above, convincing evidence for 240-pS channels that are nearly or fully open most of the time at V_j 0 and open to lower substates when $V_j \pm 80$ mV is applied is provided here in Figs. 10 and 11. In all preparations studied in the present work, over a 100-fold range in G_j (0.24–22.5 nS), a step in V_j greater than 20–30 mV in either polarity resulted in a characteristic current response, composed of an initial spike of current whose magnitude reflected the immediately prior resting conductance, followed by an exponential decay to a lower steady-state level. The size and constancy of shape of the decay over such a broad range of values of G_j argues against a current-based mechanism such as that found in the earthworm septate junction by Brink et al. (1988), as does the single-channel evidence in Figs. 10–11. Especially the biexponential decline that results from an ensemble average of the activity of a single channel allows us to discount an explanation for the decay on the basis of ion accumulation at the mouths of the junctional channels. These results confirm and extend experiments previously reported on embryonic chick (Chen et al., 1988; DeHaan et al., 1989; Veenstra, 1990*a-c*) and neonatal mammalian (Rook et al., 1988, 1989; Veenstra, 1990*a*) heart cells.

The voltage and time dependence of embryonic and neonatal junctions distinguishes them from most adult preparations, but their sensitivity to V_j varies considerably. Spray et al. (1981) demonstrated that the steady-state conductance of junctions connecting pairs of amphibian blastomeres decreased as a steep function of V_j in accordance with a Boltzmann relation. The assumptions underlying a Boltzmann fit are that G_j depends upon a homogeneous population of two-state channels, that the energy difference between the states is a linear function of V_j (in either polarity), and that transitions between the states are reversible and first order. The success in fitting our data, based on multiple-channel levels, with a Boltzmann equation of the form shown (Table 3, Fig. 6*D*) appears to be inconsistent with those assumptions. It suggests either that the equation is relatively insensitive to small differences in transition energies or that one of the transitions is substantially more energetic than the rest, and therefore, dominates in measurements of voltage sensitivity. In amphibian blastomeres the potential at half-maximal G_j (V_o) was about ±14 mV and G_{min}/G_{max} was about 0.05 at ± 30 mV. The response to a large voltage step was monoexponential and rapid with decay time constants of 200–400 msec. Interestingly, the voltage-dependent closure of junctions formed by *Xenopus* oocyte pairs injected with mRNA for connexin38, a junctional polypeptide extracted from *Xenopus* oocytes and embryos through gastrulation, was multiexponential and much less steep, with V_o at about 45 mV (Ebihara et al., 1989). The parameters of chick heart cell junctions are intermediate, showing V_o at about 40 mV and G_{min}/G_{max} near 0.3 at ±80 mV V_j (Table 3 above and Veenstra, 1990*b*, Table 3).

Our results on the voltage dependence of gap junctions and those of Veenstra's laboratory are qualitatively similar, as would be expected from what appear to be nearly identical preparations (Veenstra, 1990*c*). The two sets of data are consistent in finding that the rate of conductance decay increases with V_j. However, important differences exist between Veenstra's findings and ours. His time constants are based on monoexponential fits while ours require biexponentials (compare Table 4, *see above*, with Table 1 in Veenstra, 1990*c*). This discrepancy is presumably explained by the fact that we fit 6 sec of data for each current record, whereas Veenstra apparently truncated his records, fitting only the initial 1 sec. Another important discrepancy is that Veenstra found that the recovery of G_j after returning to 0 V_j was also monoexponential and was slow, with a time constant of 1.1 sec, while we found that recovery is also biexponential (Table 4). A multiexponential time course is consistent with our contention that the mechanism of voltage-dependent gating of embryonic junctional channels is complex and involves more than one component process.

In conclusion, we show here that the junctional channels of embryonic chick ventricle exhibit multiple conductances. We argue that these data are consistent with three models of junctional channels:

small channels that exhibit cooperativity; channels that have single large pores with substates; or a variety of channels of several different sizes. A possible explanation for our finding that conductance decay and recovery have two time constants is that the voltage sensitivity of the various channels (or states) may differ. That is, the effects of V_j on the kinetics of large channel openings may be different from its effects on the smaller channel conductances. Alternatively, the fast time constants may result from the direct effect of the applied transjunctional field on the channel voltage sensor, whereas the slower time constants may arise from indirect effects on phosphorylation of the junctional channel protein (Crow et al., 1990; Musil et al., 1990) or other enzymatically activated changes (Spray & Burt, 1990).

We thank Ms. B.J. Duke for technical assistance and for preparation of the cell cultures and Drs. L.J. DeFelice and D. Eaton for stimulating and helpful discussions of the results.

References

Bennett, M.V.L., Barrio, L.C., Bargiello, T.A., Spray, D.C., Hertzberg, E., Saez, J.C. 1991. Gap junctions: New tools, new answers, new questions. *Neuron* **6**:305–320

Beyer, E.C. 1990. Molecular cloning and developmental expression of two chick embryo gap junction proteins. *J. Biol.Chem.* **265**:14439–14443

Beyer, E.C., Paul, D.L., Goodenough, D.A. 1990. Connexin family of gap junction proteins. *J. Membrane Biol.* **116**:187–194

Brink, P.R., Fan, S.-F. 1989. Patch clamp recordings from membranes which contain gap junction channels. *Biophys. J.* **56**:579–593

Brink, P.R., Mathias, R.T., Jaslove, S.W., Baldo, G.J. 1988. Steady-state current flow through gap junctions. *Biophys. J.* **53**:795–807

Burt, J.M., Spray, D.C. 1988. Single channel events and gating behavior of the cardiac gap junction channel. *Proc. Natl. Acad. Sci. USA* **85**:3431–3434

Catterall, W.A. 1988. Structure and function of voltage-sensitive ion channels. *Science* **242**:50–61

Chen, Y.-H., DeHaan, R.L. 1989. Cardiac gap junction channels shift to lower conductance states when temperature is reduced. *Biophys. J.* **55**:152*a*

Chen, Y.-H., DeHaan, R.L. 1992. Multiple channel conductance states in gap junctions. *In:* International Gap Junction Conference. J.S. Hall and G. Zampighi, editors. Elsevier, Amsterdam (*in press*)

Chen, Y.-H., Penrod, R.L., DeHaan, R.L. 1988. Conductance of gap junctions in embryonic heart cells is voltage dependent. *Int. Congr. Cell. Biol.* **4**:234*a*

Crow, D.S., Beyer, E.C., Paul, D.L., Kobe, S.S., Lau, A.F. 1990. Phosphorylation of connexin43 gap junction protein in uninfected and rous-sarcoma virus-transformed mammalian fibroblasts. *Mol. Cell. Biol.* **10**:1754–1763

DeHaan, R.L. 1988. Dynamic behavior of cardiac gap junction channels. *In:* Gap Junctions. E. Hertzberg and R. Johnson, editors. pp. 305–320. Alan R. Liss, New York

DeHaan, R.L., Chen, Y.-H., Penrod, R.L. 1989. Voltage dependence of junctional conductance in the embryonic heart. *In:* Molecular and Cellular Mechanisms of Antiarrhythmic Agents. Luc Hondeghem, editor. pp. 19–43. Futura, Mount Kisco, New York

DeHaan, R.L., Williams, E.H., Ypey, D.L, Clapham, D.E. 1981. Intercellular coupling of embryonic heart cells. *In:* Perspectives in Cardiovascular Research. T. Pexeider, editor. pp. 299–316. Raven, New York

Ebihara, L., Beyer, E.C., Swenson, K.I., Paul, D.L., Goodenough, D.A. 1989. Cloning and expression of a *Xenopus* embryonic gap junction protein. *Science* **243**:1194–1195

Eghbali, B., Kessler, J.A., Spray, D.C. 1990. Expression of gap junction channels in communication-incompetent cells after stable transfection with cDNA encoding connexin 32. *Proc. Natl. Acad. Sci. USA* **87**:1328–1331

Fox, J.A. 1987. Ion channel subconductance states. *J. Membrane Biol.* **97**:1–8

Fujii, S., Ayer, R.K., Jr., DeHaan, R.L. 1988. Development of the fast sodium current in early embryonic chick heart cells. *J. Membrane Biol.* **101**:209–223

Giaume, C., Fromaget, C., Aoumari, A.E., Cordier, J., Glowinski, J., Gros, D. 1991. Gap junctions in cultured astrocytes: Single-channel currents and characterization of channel-forming protein. *Neuron* **6**:133–143

Godt, R.E., Lindley, B.D. 1982. Influence of temperature upon contractile activation and isometric force production in mechanically skinned muscle fibers of the frog. *J. Gen. Physiol.* **80**:279–297

Goodenough, D.A. 1976. In vitro formation of gap junction vesicles. *J. Cell Biol.* **68**:221–231

Hill, J.A., Jr., Coronado, R., Strauss, H.C. 1990. Open-channel subconductance state of K^+ channel from cardiac sarcoplasmic reticulum. *Am. J. Physiol.* **258**:H159–H164

Hunter, M., Giebisch, G. 1987. Multi-barrelled K-channels in renal tubules. *Nature* **327**:522–524

Imanaga, I., Kameyama, M., Irisawa, H. 1987. Cell-to-cell diffusion of fluorescent dyes in paired ventricular cells. *Am. J. Physiol.* **252**:H223–H232

Jahr, C.E., Stevens, C.F. 1987. Glutamate activated multiple single channel conductances in hippocampal neurons. *Nature* **325**:522–523

Jan, L.Y., Jan, Y.N. 1989. Voltage-sensitive ion channels. *Cell* **56**:13–25

Kell, M.J., DeFelice, L.J. 1988. Surface charge near the cardiac inward-rectifier channels measured from single-channel conductance. *J. Membrane Biol.* **102**:1–10

Kolb, H.-A., Somogyi, R. 1990. Characteristics of single channels of pancraetic acinar gap junctions subject to different uncoupling procedures. *In:* Biophysics of Gap Junction Channels. C. Peracchia, editor. pp. 209–228. CRC Press, Boca Raton (FL)

Läuger, P. 1985. Ionic channels with conformational substates. *Biophys. J.* **47**:581–591

Loewenstein, W.R. 1981. Junctional intercellular communication: The cell-to-cell membrane channel. *Physiol. Rev.* **61**:829–913

Millhauser, G.L. 1990. Reptation theory of ion channel gating. *Biophys. J.* **57**:857–864

Moreno, A.P., Campos de Carvalho, A.C., Verselis, V., Eghbali, B., Spray, D.C. 1991. Voltage-dependent gap junction channels are formed by connexin32, the major gap junction protein of rat liver. *Biophys. J.* **59**:920–925

Musil, L.S., Beyer, E.C., Goodenough, D.A. 1990. Expression

of the gap junction protein connexin43 in embryonic chick lens: Molecular cloning, ultrastructural localization, and post-translational phosphorylation. *J. Membrane Biol.* **116:**163–175

Noma, A., Tsuboi, N. 1987. Dependence of junctional conductance on proton, calcium and magnesium ions in cardiac paired cells of guinea-pig. *J. Physiol.* **382:**193–211

Page, E., Manjunath, C.K. 1986. Communicating junctions between cardiac cells. *In:* The Heart and Cardiovascular System. H.A. Fozzard, E. Haber, R.B. Jennings and H.E. Morgan, editors. pp. 573–600. Raven, New York

Patlak, J. 1991. Molecular kinetics of voltage-dependent Na^+ channels. *Physiol. Rev.* **71:**1047–1080

Rook, M.B., Jongsma, H.J., de Jonge, B. 1989. Single channel currents of homo- and heterologous gap junctions between cardiac fibroblasts and myocytes. *Pfluegers Arch.* **414:**95–98

Rook, M.B., Jongsma, H.J., van Ginneken, 1988. Properties of single gap junctional channels between isolated neonatal rat heart cells. *Am. J. Physiol.* **255:**H770–H782

Rudisuli, A., Weingart, R. 1990. Gap junctions in adult ventricular muscle. *In:* Biophysics of Gap Junction Channels. C. Peracchia, editor. pp. 43–56. CRC Press, Boca Raton (FL)

Sakmann, B., Trube, G. 1984. Voltage-dependent inactivation of inwardly-rectifying single-channel currents in guinea pig ventricle. *J. Physiol.* **347:**659–683

Schindler, H. 1989. Planar lipid-protein membranes: Strategies of formation and of detecting dependencies of ion transport functions on membrane conditions. *Methods Enzymol.* **171:**225–253

Schwarzmann, G., Wiegandt, H., Rose, B., Zimmerman, A., Ben-Haim, D., Loewenstein, W.R. 1981. Diameter of the cell-to-cell junctional channels as probed with neutral molecules. *Science* **213:**551–553

Somogyi, R., Kolb, H.-A. 1988.Cell-to-cell channel conductance during loss of gap junctional coupling in pairs of pancreatic acinar and Chinese hamster ovary cells. *Pfluegers Arch.* **412:**54–65

Spray, D.C., Bennett, M.V.L., Campos de Carvalho, A.C., Eghbali, B., Moreno, A.P. Verselis, V. 1990. Transjunctional voltage dependence of gap junction channels. *In:* Biophysics of Gap Junction Channels. C. Peracchia, editor. pp. 97–116. CRC Press, Boca Raton (FL)

Spray, D.C., Burt, J.M. 1990. Structure-activity relations of the cardiac gap junction channel. *Am. J. Physiol.* **258:**C195–C205

Spray, D.C., Harris, A.L., Bennett, M.V.L. 1981. Equilibrium properties of a voltage-dependent junctional conductance. *J. Gen. Physiol.* **77:**77–93

Swenson, K.I., Jordan, J.R., Beyer, E.C., Paul, D.L. 1989. Formation of gap junctions by expression of connexins in *Xenopus* oocyte pairs. *Cell* **57:**145–155

Unwin, N. 1989. The structure of ion channels in membranes of excitable cells. *Neuron* **3:**665–676

Veenstra, R.D. 1990*a*. Comparative physiology of cardiac gap junction channels. *In:* Biophysics of Gap Junction Channels. C. Peracchia, editor. pp. 131–144. CRC Press, Boca Raton (FL)

Veenstra, R.D. 1990*b*. Voltage-dependent gating of gap junctional conductance in embryonic chick heart. *Ann. NY Acad. Sci.* **588:**93–105

Veenstra, R.D. 1990*c*. Voltage-dependent gating of gap junction channels in embryonic chick ventricular cell paris. *Am. J. Physiol.* **285:**C662–C672

Veenstra, R.D., DeHaan, R.L. 1988. Cardiac gap junction channel activity in embryonic chick ventricle cells. *Am. J. Physiol.* **254:**H170–H180

Veenstra, R.D., Wang, H.-Z., Westphale, E.M., Beyer, E.C. 1991. Functional differences between embryonic chick heart connexins. *J. Cell Biol.* **115:**191*a*

Verselis, V., White, R.L., Spray, D.C., Bennett, M.V.L. 1986. Gap junctional conductance and permeability are linearly related. *Science* **234:**462–464

Werner, R., Levine, E., Rabadan-Diehl, C., Dahl, G. 1989. Formation of hybrid cell-cell channels. *Proc. Natl. Acad. Sci. USA* **86:**5380–5384

Yellen, G. 1984. Ionic permeation and blockade in Ca^{2+}-activated K^+ channels of bovine chromaffin cells. *J. Gen. Physiol.* **84:**157–186

Young, J.D.-E., Cohn, Z.A., Gilula, N.B. 1987. Functional assembly of gap junction conductance in lipid bilayers: Demonstration that the major 27 kD protein forms the junctional channel. *Cell* **48:**733–743

Zimmerman, A.L., Rose, B. 1985. Permeability properties of cell-to-cell channels: Kinetics of fluorescent tracer diffusion through a cell junction. *J. Membrane Biol.* **84:**269–283

Received 10 September 1991; revised 22 November 1991